The theory of the longitudinal development of electromagnetic cascades

1972 J. Phys. A: Gen. Phys. 5 1054

(http://iopscience.iop.org/0022-3689/5/7/015)

J. Phys. A: Gen. Phys., Vol. 5, July 1972. Printed in Great Britain.

The theory of the longitudinal development of electromagnetic cascades

K O THIELHEIM and R ZÖLLNER

University of Kiel, Gebaude 32, Germany

MS received 29 November 1971

Abstract. A method for the numerical integration of the cascade equations of the longitudinal development of electromagnetic cascades is described. Numerical results on the longitudinal development of electron induced cascades in lead are presented in graphical form. Comparisons with data from Monte Carlo simulations and with experimental data are presented. The accuracy of approximations A and B of conventional cascade theory is investigated.

1. Historical background

The conventional theory of electromagnetic cascade development is mainly based on the application of Laplace and Mellin transforms to a system of transport equations. After the pioneer work of Carlson and Oppenheimer (1937), Bhabha and Heitler (1937) and Landau and Rumer (1938), who introduced this method for the calculation of longitudinal cascade development without ionization losses and its improvement by Snyder (1938) and Bhabha and Chakrabarthy (1943) who included ionization losses in this treatment, conventional cascade theory has continuously been further developed by Snyder (1949), Bhabha and Chakrabarthy (1948), Nishimura and Kamata (1952), Chakrabarthy and Gupta (1956) and many other authors.

An alternative approach to the numerical treatment of the cascade problem was offered by the Monte Carlo method first applied by Wilson (1952) especially after the invention of electronic computers. A great amount of data have become available from the work of Butcher and Messel (1960), Zerby and Moran (1963) and Nagel (1965).

Recently, a method for the numerical integration of cascade equations on the basis of 'exact' cross sections has been proposed (Thielheim and Zöllner 1970a) which may be useful in view of the widespread application of electromagnetic cascade theory in high energy and cosmic ray physics. These results do not suffer from difficulties inherent either in conventional cascade theory due to the application of asymptotic cross sections and approximative procedures or in Monte Carlo simulations, namely the statistical fluctuations of results and the linear increase of computing time with increasing initial energy.

In this paper, after a presentation of cascade equations and fundamental cross sections, the method of numerical integration is described in detail together with results on the longitudinal development of electron induced cascades in lead. These results, which are estimated to be accurate to about 1 % in a specified region of energy enable us to analyse deficiencies of approximations A and B of conventional cascade theory.

2. Cascade equations

The mean longitudinal development of electromagnetic cascades is described by a set of distribution functions $F(j, E_0, E, t)\,\mathrm{d}E$ giving the mean number of particles of type j within the range of energy $(E, E+\mathrm{d}E)$ at the depth t within a cascade of primary energy E_0. These distribution functions are obtained as solutions of a system of integrodifferential equations with given initial conditions.

The system of cascade equations expresses the change in the mean numbers of particles of type j within the range of energy $(E, E+\mathrm{d}E)$ in the interval of depth $(t, t+\mathrm{d}t)$

$$\frac{\partial}{\partial t}F(j,E_0,E,t) = \lim_{\eta\to 0}\left(\sum_k \int_{E+\eta}^{E_0} \mathrm{d}E'\, W^{k\to j}(t,E',E)F(k,E_0,E',t)\right.$$
$$\left.-\sum_k \int_0^{E-\eta} \mathrm{d}E'\, W^{j\to k}(t,E,E')F(j,E_0,E,t)\right) + S^j(t,E) \qquad \text{for } j=1,\ldots,N. \tag{2.1}$$

This expression contains positive contributions originating from interactions within energy intervals $(E', E'+\mathrm{d}E')$ above the energy E considered as well as negative contributions describing the loss of particles of type j within the range of energy $(E, E+\mathrm{d}E)$, in the interval $(t, t+\mathrm{d}t)$. $W^{j\to k}(t, E, E')\,\mathrm{d}E'\,\mathrm{d}t$ is the probability for a particle of type j and energy E to give rise to a particle of type k within the range of energy $(E', E'+\mathrm{d}E')$ in the interval $(t, t+\mathrm{d}t)$. The quantity $S^j(t, E)$ is an additional source term.

Introducing N-component functions $f(E, t)$ and $S(E, t)$, as well as the square matrix W of N rows corresponding to the number N of different types of particles and the diagonal matrix $\tilde{W}$, the system of cascade equations with respect to different components is written in matrix form

$$\frac{\partial}{\partial t}F(E,t) = \lim_{\eta\to 0}\left(\int_{E+\eta}^{E_0} \mathrm{d}E'\, W(t,E',E)F(E',t) - \int_0^{E-\eta} \mathrm{d}E'\, \tilde{W}(t,E,E')F(E,t)\right) + S(E,t). \tag{2.2}$$

3. Cross sections

The following fundamental interactions are taken into account: bremsstrahlung, Møller scattering and Bhabha scattering (at high energy transfer), ionization (at low energy transfer), pair production, photoeffect and Compton scattering. Interaction probabilities are used in the form of first order Born approximations of quantum electrodynamics with various corrections. Explicit formulae are presented in table 1 (units of energy are $mc^2 = 1$).

The formula of the differential probability for bremsstrahlung implies atomic shielding corrections based on the Thomas–Fermi model. Corrections are also provided for particles outgoing in a Coulomb field. Additionally, there is an empirical correction factor, which depends only on the initial energy and the atomic number. This correction factor is shown in figure 1 for illustration. The asymptotic form of this formula is obtained for complete screening and the neglection of Coulomb as well as empirical correction terms.

The differential probability for pair production implies the same atomic shielding and Coulomb correction functions. The empirical correction factor, as shown in figure 1, depends only on the initial energy and the atomic number. Again, the asymptotic form is obtained for complete screening and neglection of Coulomb as well

Table 1. Explicit formulae for the fundamental interaction probabilities

Bremsstrahlung

Probability per GeV per radiation length

$$\frac{f_{br}(E,E_f)}{E}=\frac{1}{E-E_f}\left[\left\{1+\left(\frac{E_f}{E}\right)^2\right\}(1+F_1(\delta))-\frac{2}{3}\frac{E_f}{E}(1+F_2(\delta))\right]C_{br}(E,Z)$$

E: initial, E_f: final energy of electron; $C_{br}(E,Z)$: empirical correction factor[a]; asymptotic form for lead: $\chi(V)=\{1{\cdot}36(1-V)+V^2\}/V$, where $V=E_f/E$;

screening parameter[b] $\delta=\dfrac{136}{Z^{1/3}}\dfrac{E-E_f}{EE_f}$

The following definitions apply throughout the table:

Thomas–Fermi screening functions

$$\left.\begin{aligned}F_1(\delta)&=\{(-3{\cdot}24\delta+0{\cdot}625\delta^2)/4-f(Z)\}/\ln(183Z^{-1/3})\\F_2(\delta)&=\{(-\tfrac{2}{3}-1{\cdot}93\delta-0{\cdot}086\delta^2)/4-f(Z)\}/\ln(183Z^{-1/3})\end{aligned}\right\}\delta\leqslant 1$$

$$F_1(\delta)=F_2(\delta)=[\{0{\cdot}2-4{\cdot}18\ln(\delta-0{\cdot}952)\}/4-f(Z)]/\ln(183Z^{1/3})\qquad\delta>1$$

where the Coulomb correction[c]

$$f(Z)=(\alpha Z)^2\sum_{j=1}^{\infty}1/[j\{j^2+(\alpha Z)^2\}]$$

Radiation length ($g\,cm^{-2}$)

$$t_0=\frac{1}{4\alpha r_0^2 Z(Z+\xi)(N/\rho)\ln(183Z^{-1/3})}$$

where

$$\xi=\frac{\ln(1440Z^{-2/3})}{\ln(183Z^{-1/3})}$$

Pair production

$$\frac{f_p(E,E^+)}{E}=\frac{1}{E^3}[\{E^{+2}+(E-E^+)^2\}(1+F_1(\delta))+\tfrac{2}{3}E^+(E-E^+)(1+F_2(\delta))]C_p(E,Z)$$

E: initial photon energy; E^+: final positron energy; $C_p(E,Z)$: empirical correction factor[d]; asymptotic form for lead: $\chi(V)=1-1{\cdot}36(1-V)$, where $V=E^+/E$;

screening parameter[b] $\delta=\dfrac{136}{Z^{1/3}}\dfrac{E}{E^+E^-}$

Møller scattering[e]

$$\frac{f_M(E,E_f)}{T}=\frac{1}{T^2}\left\{\frac{1}{V^2}+\frac{1}{(1-V)^2}+\left(\frac{T}{E}\right)^2-\frac{2T+1}{E^2}-\frac{1}{V(1-V)}\right\}C_M(E)$$

$V=T_f/T$; $T=E-1$; $T_f=E_f-1$; $C_M(E)=\pi/\{2\alpha(Z+\xi)\ln(183Z^{-1/3})\beta^2\}$

Table 1—continued

Bhabha scattering[f]

$$\frac{f_{Bh}(E, E_f)}{T} = \frac{1}{T^2}\left\{\frac{1}{V^2} - \beta^2\left(\frac{A}{V} + B + CV + DV^2\right)\right\} C_M(E)$$

$V = T_f/T$; $A = 2 - y^2$; $B = -(3 - 6y + y^2 - 2y^3)$; $C = 2 - 10y + 16y^2 - 8y^3$; $D = -(1 - 6y + 12y^2 - 8y^3)$, where $y = 1/(T+2)$

Ionization loss[g]

Mean energy per radiation length

$$-\frac{dE}{dt} = C_M(E)\left\{\ln\left(\frac{\beta^2 W}{I^2(1-\beta^2)}\right) - \{2(1-\beta^2)^{1/2} - (1-\beta^2)\ln(2)\} + (1-\beta^2) + \tfrac{1}{8}\{1-(1-\beta^2)^{1/2}\}^2 - \delta\right\}$$

W: maximal energy transferred to secondary; I: mean ionization potential

Correction for density effect[h]

$$\delta = \begin{cases} 0 & X < 1{\cdot}75 \\ X - 6{\cdot}03 - 0{\cdot}316(3 - X/4{\cdot}608)^{2{\cdot}71} & 1{\cdot}75 < X < 13{\cdot}82 \\ X - 6{\cdot}03 & 13{\cdot}82 < X \end{cases} \qquad \text{where } X = -\ln(1/\beta^2 - 1)$$

Compton scattering[i]

$$\frac{f_c(E, E_f)}{E} = \frac{\pi}{4\alpha(Z+\xi)\ln(183Z^{-1/3})}\frac{1}{E^3}\left\{\frac{E}{E_f} + \frac{E_f}{E} - 2\left(\frac{1}{E_f} - \frac{1}{E}\right) + \left(\frac{1}{E_f} - \frac{1}{E}\right)^2\right\}$$

E: initial, E_f: final photon energy

Photoelectric effect

$$\frac{f_{ph}(E, E_f)}{E} = \frac{\pi Z^5 \alpha^3}{(Z+\xi)\ln(183Z^{-1/3})}\frac{\delta(E - E_f)}{E^6}(\gamma^2 - 1)^{3/2}\left\{\frac{4}{3} + \frac{\gamma(\gamma-2)}{\gamma+1}\left(1 - \frac{1}{2\gamma(\gamma^2-1)^{1/2}}\ln\left\{\frac{\gamma + (\gamma^2-1)^{1/2}}{\gamma - (\gamma^2-1)^{1/2}}\right\}\right)\right\} F_H(Z) C_{ph}(E)$$

$\gamma = E + 1$; E: initial photon energy; E_f: final electron energy; $F_H(Z) = \exp[-\pi Z\alpha + 2(Z\alpha)^2\{1 - \ln(Z\alpha)\}]$ (see footnote j); C_{ph}: empirical correction factor[d]

[a] Koch and Motz (1959); [b] Butcher and Messel (1960); [c] Davis *et al* (1954); [d] Grodstein (1957); [e] Møller (1932); [f] Bhabha (1936); [g] Bethe and Ashkin (1953); [h] Sternheimer (1952); [i] Klein and Nishina (1929); [j] Hall (1936).

as empirical corrections. The energy loss of an electron due to electron–electron scattering is understood as an individual interaction if the energy loss exceeds 0·1 MeV. These collisions are described by Møller's formula.

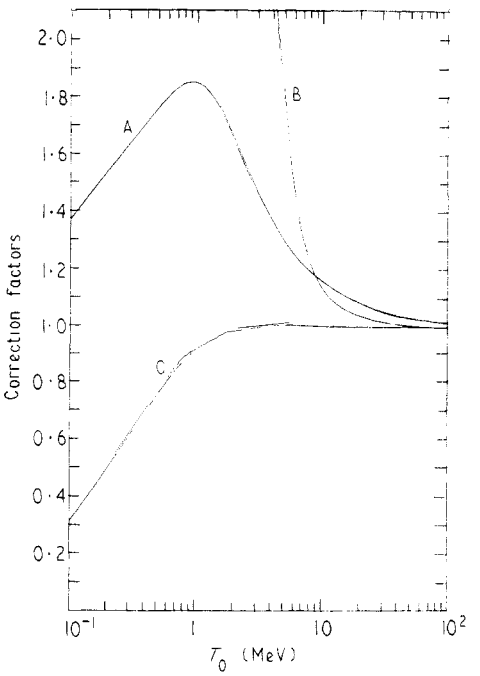

Figure 1. Empirical correction factors, A : $C_{br}(E, Z)$, B : $C_p(E, Z)$ and C : $C_{ph}(E, Z)$, as functions of energy T for lead ($Z = 82$).

Similarly, the energy loss of a positron due to positron–electron scattering is understood as an individual interaction if the energy loss exceeds 0·1 MeV. These collisions are described by Bhabha's formula. In both cases knock-on particles are taken into account. (In the calculations, the results of which are presented below, Møller's formula is used if the initial energy is smaller than 10 MeV, while Møller's and Bhabha's formulae are used with weight one half each, if the initial energy is greater than 100 MeV. In the region of initial energy between 10 MeV and 100 MeV a linear interpolation of both formulae is applied.) If the energy loss of electrons or positrons in electron–positron collisions or positron–electron collisions, respectively, is smaller than 0·1 MeV the interaction is described as a continuous process, in which the density effect is taken into account. (The results given in this paper have been calculated using the expression for the ionization loss of electrons for both electrons and positrons, since at low energies the number of electrons is much greater than the number of positrons while at high energies the expressions for the energy loss of electrons and of positrons coincide.) The energy loss of photons due to Compton scattering is described by means of the well known formula of Klein and Nishina.

The interaction probability for the photoeffect is dealt with by means of Sauter's formula with empirical corrections in the low energy region as is illustrated in figure 1.

4. Numerical procedure

Discrete intervals of geometrically increasing length $T_{g+1} = (1+\alpha)T_g$ with $0 \leqslant \alpha \leqslant 1$ and $g = 1, \ldots, M$ are introduced for numerical integration with respect to 'kinetic' energy $T = E$ for photons and $T = E-1$ for electrons. (Calculations have been performed with $1+\alpha = 10^{1/16}$; the unit of energy is $mc^2 = 1$.)

Any function $F(T)$ is represented by mean values F^g. Mean values $W^{g,g'}$ of $W(T, T')$ are calculated from

$$W^{g,g'} = \frac{1}{T_{g+1}-T_g} \int_{T_g}^{T_{g+1}} \frac{\mathrm{d}T}{T_{g'+1}-T_{g'}} \int_{T_{g'}}^{T_{g'+1}} \mathrm{d}T'\, W(T, T')G(T') \tag{4.1}$$

with the help of a weight function $G(T) \propto 1/(T+\text{constant})^m$ with $1 \leqslant m \leqslant 3$, the parameters of which are chosen to give an approximative representation $F(T) \simeq F^g G(T)$ within each interval (T_g, T_{g+1}). The relative error induced by this procedure

$$\left(\frac{1}{T_{g+1}-T_g}\int_{T_g}^{T_{g+1}} \mathrm{d}T \frac{1}{T_{g'+1}-T_{g'}} \int_{T_{g'}}^{T_{g'+1}} \mathrm{d}T'\, W(T, T')F(T') - W^{g,g'}F^{g'}\right)(W^{g,g'}F^{g'})^{-1} \tag{4.2}$$

is estimated to be smaller than

$$\frac{1}{3}\left(\frac{T_{g'+1}-T_{g'}}{T_{g'}}\right)^2. \tag{4.3}$$

The choice of geometrically increasing intervals results in the proportionality of computing time to $\ln T_0$. By discretization with respect to energy, the cascade equations (2.2) are reduced to a system of ordinary differential equations with respect to depth

$$\frac{\mathrm{d}}{\mathrm{d}t}F^g(t) = \sum_{g'=g}^{M} W^{g,g'}(t)F^{g'}(t) + S^g(t). \tag{4.4}$$

More economically, these equations are written in matrix notation also with respect to different groups of energy

$$\frac{\mathrm{d}}{\mathrm{d}t}F(t) = W(t)F(t) + S(t). \tag{4.5}$$

If the matrix W is independent of depth, as is assumed in the following considerations, the solution of this equation for given initial values $F_0 = F(t_0)$ is

$$F(t) = \exp\{W \,.\, (t-t_0)\} \,.\, F_0 + \int_{t_0}^{t} \mathrm{d}t' \exp\{W \,.\, (t-t')\}S(t'). \tag{4.6}$$

In the absence of 'external sources' $S(t)$ the solution is

$$F(t) = \exp\{W \,.\, (t-t_0)\}F_0 \tag{4.7}$$

which may be calculated numerically by approximative procedures. For small values of the elements of the argument matrix $W \,.\, \Delta t$ the matrix exponential function $\exp(W \,.\, \Delta t)$ is approximated to the second order by

$$\exp(W \,.\, \Delta t) \simeq \left(1 - \frac{W \,.\, \Delta t}{2}\right)^{-1} \,.\, \left(1 + \frac{W\Delta t}{2}\right). \tag{4.8}$$

The difference matrix is obviously of the order of

$$\tfrac{1}{12}(W \,.\, \Delta t)^3. \tag{4.9}$$

For greater values of the elements of the argument matrix $(W \cdot \Delta t)$ the approximation (4.8) is written in the form

$$\exp(W \cdot \Delta t) = \left\{ \exp\left(W \cdot \frac{\Delta t}{\kappa} \right) \right\}^{\kappa}$$

$$\simeq \left\{ \left(1 - W \cdot \frac{\Delta t}{2\kappa} \right)^{-1} \left(1 + W \cdot \frac{\Delta t}{2\kappa} \right) \right\}^{\kappa} . \tag{4.10}$$

The number κ of subintervals within the range Δt is determined from the limit of the error admitted. For example, if the range is $t = 40\, X_0$ for an error smaller than 0·1 %, the number of subintervals is found to be $\kappa = 2 \times 10^3$. (Results presented below have been obtained with $\kappa = 8 \times 10^3$ intervals.)

5. Results

In figure 2(*a*, *b*, *c* and *d*) integral energy spectra $N_e(T > T_c, t)$ of electrons in electron induced electromagnetic cascades in lead are represented in the form of 'transition curves' as functions of depth t (in units of radiation length). Initial energies are $T_0 = 10^3$ MeV, 10^4 MeV, 10^5 MeV, and 10^6 MeV. In each diagram, different curves correspond to different values of cut-off energy T_c. Curves for cut-off energies $T_c \leqslant 10$ MeV should be corrected due to the lateral divergence of particles.

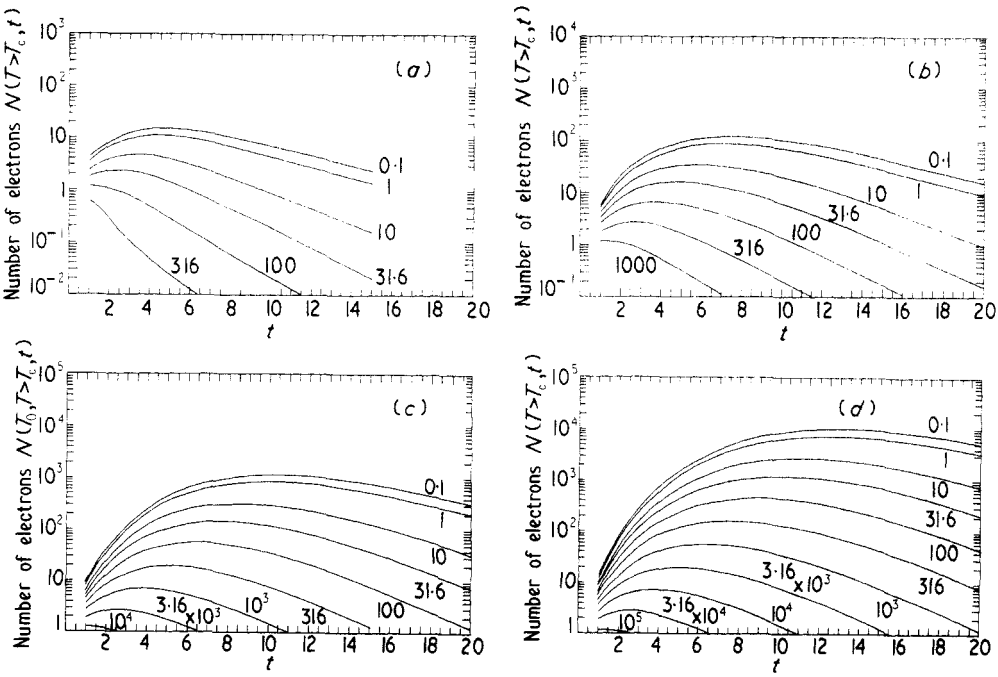

Figure 2. Transition curves $N_e(T > T_c, t)$ of electrons in electron induced cascades in lead for four values of T_0 (MeV): (*a*) 10^3, (*b*) 10^4, (*c*) 10^5 and (*d*) 10^6. In each part, different curves correspond to different values of T_c (MeV).

In figure 3(*a*, *b*, *c* and *d*), analogously, 'transition curves' for photons are shown. In the range of small depth, these curves exhibit the well known increase with increasing

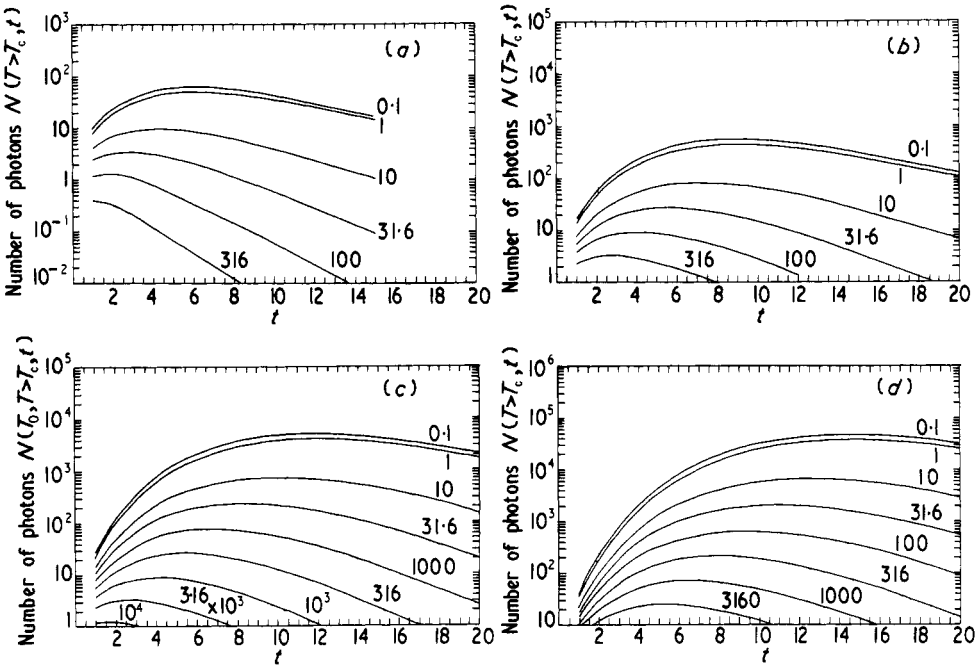

Figure 3. Transition curves $N_\gamma(T > T_c, t)$ of photons in electron induced cascades in lead for four values of T_0 (MeV): (*a*) 10^3, (*b*) 10^4, (*c*) 10^5 and (*d*) 10^6. In each part, different curves correspond to different values of T_c (MeV).

Table 2. Interpolating formulae

Max $N_e(T_0, T_c)$, $t^e_{max}(T_0, T_c)$, max $N_\gamma(T_0, T_c)$, $t^\gamma_{max}(T_0, T_c)$ concerning electron induced electromagnetic cascades in lead

$$\text{Max } N_e(T_0, T_c) = \left(V\frac{1+10\,V}{\{1+(5{\cdot}15/T_c)\}14{\cdot}55}\right)^{0{\cdot}936}$$

$$\text{Max } N_\gamma(T_0, T_c) = \left\{V\frac{1+6{\cdot}61V+61V^2}{11{\cdot}5(1+61V^2)}\left(1+\frac{1}{2}\frac{\ln(T_c)}{T_c}\right)\right\}^{0{\cdot}97}$$

$$t^e_{max}(T_0, T_c) = 1{\cdot}086\ln\left(\frac{V}{\{1+(2{\cdot}36/T_c)\}3{\cdot}185}\right)$$

$$t^\gamma_{max}(T_0, T_c) = \begin{cases} 0{\cdot}74V^{0{\cdot}359} & 3{\cdot}16 \leqslant V \leqslant 10^2 \\ \dfrac{2{\cdot}7}{2{\cdot}304}\ln(V)-1{\cdot}4 & V > 10^2 \end{cases}$$

$$V = \frac{T_c}{T_0}$$

$$\text{Range of validity}\begin{cases} 100\text{ MeV} \leqslant T_0 \leqslant 10^6\text{ MeV} \\ 10\text{ MeV} \leqslant T_c \leqslant 10^5\text{ MeV} \\ \text{and} \qquad V \leqslant 0{\cdot}1 \end{cases}$$

Inaccuracy less than 10%

depth as a consequence of particle multiplication due to pair production and bremsstrahlung. At a certain value of depth $t^{e}_{max}(T_0, T_c)$ or $t^{\gamma}_{max}(T_0, T_c)$ a curve may pass through a maximum: max $N_e(T_0, T_c)$ or max $N_\gamma(T_0, T_c)$, respectively. These parameters of 'transition curves' are reproduced by interpolative formulae in table 2. In the range of great depth, integral particle numbers decrease exponentially with increasing depth. The exponential coefficient λ_c is determined through the equilibrium of particle production and absorption.

In figure 4(*a* and *b*) differential energy spectra $\Pi(T_0, T, t)$ of electrons are shown as functions of depth for initial energies $T_0 = 10^3$ MeV, and 10^6 MeV. In each diagram, different curves refer to different values of depth. In the range of energy $T \leqslant 10$ MeV, curves should be corrected due to the obliqueness of particle trajectories.

In figure 5(*a* and *b*) differential energy spectra of photons are shown.

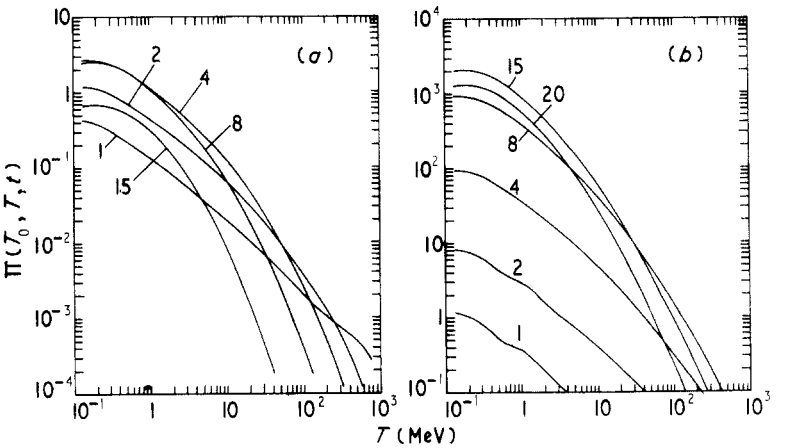

Figure 4. Differential energy spectra $\Pi(T_0, T, t)$ of electrons in electron induced cascades for two values of T_0 (MeV): (*a*) 10^3 and (*b*) 10^6. In each part, different curves correspond to different values of t (depth).

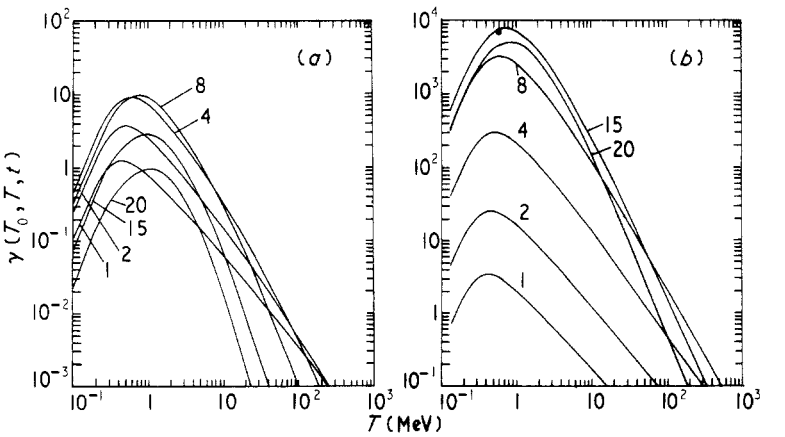

Figure 5. Differential energy spectra $\gamma(T_0, T, t)$ of photons in electron induced cascades for two values of T_0 (MeV): (*a*) 10^3 and (*b*) 10^6. In each part, different curves correspond to different values of t (depth).

6. Comparison with results of Monte Carlo simulations and with empirical data

In figures 6 to 8 our results are compared with data from Monte Carlo simulations and with empirical data (Thielheim and Zöllner 1970a, b). Integral energy spectra $N_e(T > T_c, t)$ of electrons in electron induced electromagnetic cascades in lead are shown as functions of initial energy T_0. In each diagram, different curves representing our results correspond to different values of cut-off energy T_c. Full symbols represent results of Monte Carlo simulations which have been performed by various authors on the basis of cross sections compatible with ours. Open symbols represent experimental results. In performing this comparison, one has to keep in mind that the results of Monte Carlo simulations are subject to statistical fluctuations as indicated in figure 15. Empirical results may be subject to systematic errors from the difficulty to determine the exact cut-off energy defined by the registrating apparatus.

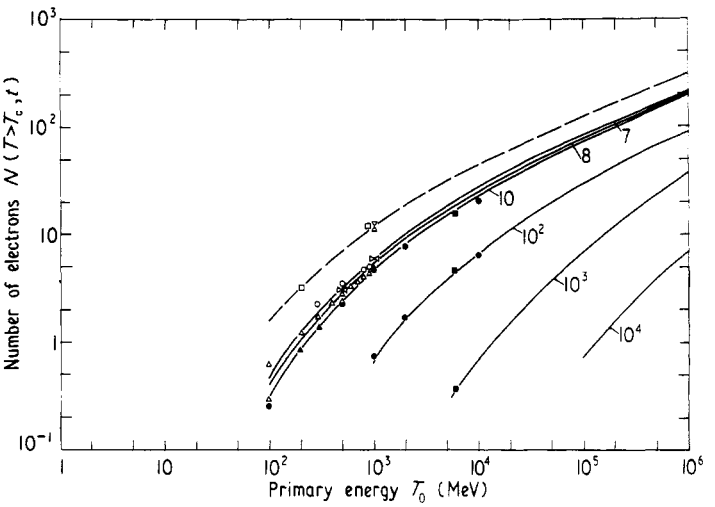

Figure 6. Integral energy spectra $N_e(T > T_c, t)$ of electrons in electron induced cascades in lead as functions of initial energy T_0 at depth $t = 3$ radiation lengths. Different curves correspond to different values of T_c (MeV). Monte Carlo data: ■ Völkel (1965); ▲ Zerby and Moran (1963); ● Messel and Crawford (1970). Experimental data: △ Heusch and Prescott (1964); ○ Thom (1964); ⋈ Becklin and Earl (1964); □ Crannel (1967); ⧖ Nelson *et al* (1966).

Obviously, there is fair agreement of our results with those from Monte Carlo simulations as well as with those from measurements, in the range of energy above several MeV, where no differences are expected between the results of one dimensional and three dimensional cascade theory.

7. Comparison of results of numerical integration with those of various approximative methods

7.1. Implications of approximations A and B of conventional cascade theory

In order to come to conclusions about the influence of simplifications involved in the application of asymptotic cross sections frequently used in approximations A and B

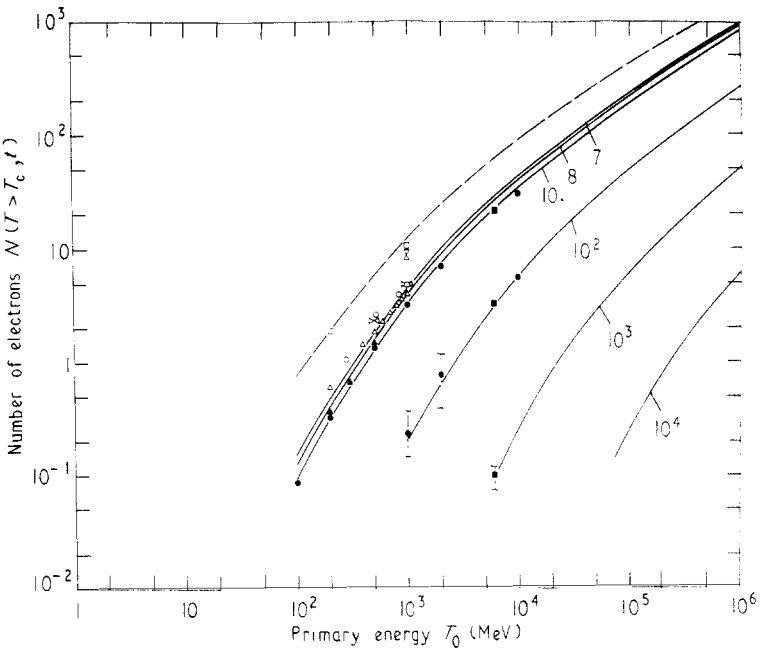

Figure 7. Integral energy spectra $N_e(T > T_c, t)$ of electrons in electron induced cascades in lead as functions of initial energy T_0 at depth $t = 5$ radiation lengths. Different curves correspond to different values of T_c (MeV). Experimental points are as described in figure 6.

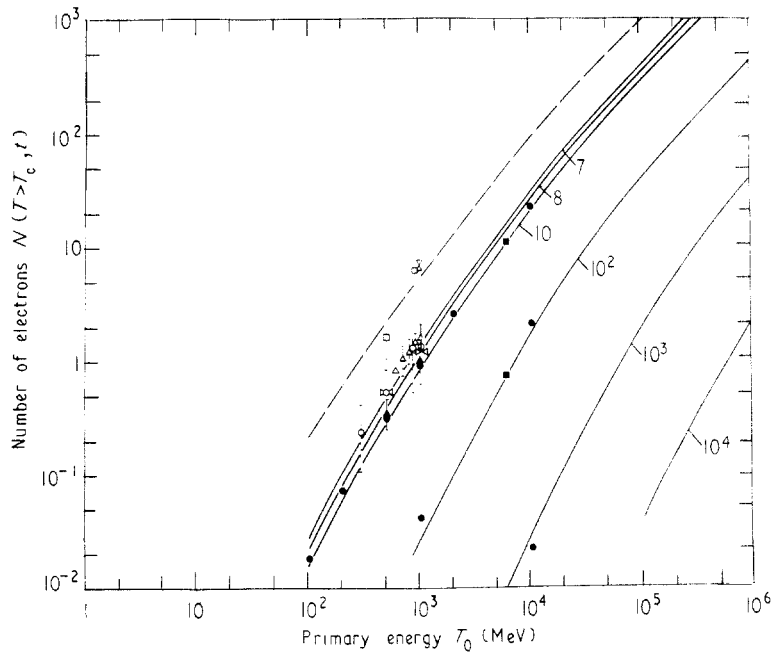

Figure 8. Integral energy spectra $N_e(T > T_c, t)$ of electrons in electron induced cascades in lead as functions of initial energy T_0 at depth $t = 9$ radiation lengths. Different curves correspond to different values of T_c (MeV). Experimental points are as described in figure 6.

of conventional cascade theory we have compared results of numerical integrations performed on the basis of asymptotic cross sections with those performed on the basis of exact cross sections (Thielheim and Zöllner 1971b).

The use of asymptotic cross sections implies the neglection of Möller and Bhabha scattering in one cascade equation and the neglection of Compton scattering and the photo effect in the other cascade equation. Moreover, in approximation B constant ionization loss is assumed as well as complete screening in pair production and bremsstrahlung. There are no empirical corrections for energies smaller than 10 MeV. In approximation A ionization loss is neglected.

In order to come to conclusions about the influence of approximative procedures involved in approximation B, we have also compared results of numerical integrations based on asymptotic cross sections with results of approximation B of cascade theory based on the same cross sections. Approximative procedures include the use of incomplete solutions by neglection of higher order terms in some series expansions and the use of the double saddle point method in integral retransformations. Finally a comparison of results from approximations A and B is performed.

7.2. Review of approximation A

We find it useful to present short reviews of approximations A and B of conventional cascade theory. In these, the differential energy spectra Π and γ of electrons and photons respectively are written as functions of total energy E rather than 'kinetic' energy T.

Under the assumptions of approximation A cascade equations reduce to the form

$$\begin{aligned} \frac{\hat{c}}{\hat{c}t}\Pi &= -A'\Pi + B'\gamma \\ \frac{\hat{c}}{\hat{c}t}\gamma &= C'\Pi - \sigma\gamma \end{aligned} \tag{7.1}$$

with integral operators

$$A'\Pi = \int_0^1 \left(\Pi(E) - \frac{1}{1-v}\Pi\left(\frac{E}{1-v}\right)\right)\phi(v)\,\mathrm{d}v \tag{7.2a}$$

$$B'\gamma = 2\int_0^1 \gamma\left(\frac{E}{v}\right)\psi(v)\frac{\mathrm{d}v}{v} \tag{7.2b}$$

$$C'\Pi = \int_0^1 \Pi\left(\frac{E}{v}\right)\phi(v)\frac{\mathrm{d}v}{v}. \tag{7.2c}$$

Making use of the homogeneity in the energy dependence, Mellin transforms are introduced

$$\begin{aligned} \Pi(E,t) &= \frac{1}{2\pi\mathrm{i}}\int_{s_0-\mathrm{i}\infty}^{s_0+\mathrm{i}\infty} \mathrm{d}s\, E^{-(s+1)} M_\Pi(s,t) \\ \gamma(E,t) &= \frac{1}{2\pi\mathrm{i}}\int_{s_0-\mathrm{i}\infty}^{s_0+\mathrm{i}\infty} \mathrm{d}s\, E^{-(s+1)} M_\gamma(s,t) \end{aligned} \tag{7.3}$$

for which the following system of ordinary differential equations holds:

$$\begin{aligned}\frac{\mathrm{d}}{\mathrm{d}t}M_{\Pi}(s,t) &= -A(s)\,.\,M_{\Pi}+B(s)\,.\,M_{\gamma}\\ \frac{\mathrm{d}}{\mathrm{d}t}M_{\gamma}(s,t) &= C(s)M_{\Pi}-\sigma\,.\,M_{\gamma}.\end{aligned} \tag{7.4}$$

The coefficients of this system of ordinary differential equations with respect to t are

$$A(s) = 1{\cdot}3603\chi(s)-\frac{1}{(s+1)(s+2)}-0{\cdot}07513 \tag{7.5a}$$

$$B(s) = \frac{2}{s}-\frac{2{\cdot}706}{(s+2)(s+3)} \tag{7.5b}$$

$$C(s) = \frac{1}{s+2}+\frac{1{\cdot}3603}{s(s+1)}. \tag{7.5c}$$

Introduction of initial conditions results in solutions

$$\begin{aligned}M_{\Pi}(s,t) &= a_1^{\Pi}(s)\,.\,\exp(\lambda_1(s)\,.\,t)+a_2^{\Pi}(s)\,.\,\exp(\lambda_2(s)\,.\,t)\\ M_{\gamma}(s,t) &= a_1^{\gamma}(s)\,.\,\exp(\lambda_1(s)\,.\,t)+a_2^{\gamma}(s)\,.\,\exp(\lambda_2(s)\,.\,t).\end{aligned} \tag{7.6}$$

The exponents λ_1 and λ_2 are determined by the conditions of solubility

$$\lambda_{1,2}(s) = -\frac{A(s)+\sigma}{2}\pm\tfrac{1}{2}\{(A(s)-\sigma)^2+4B(s)\,.\,C(s)\}^{1/2}. \tag{7.7}$$

In (7.6), the coefficients of exponential functions are determined by initial conditions

$$\begin{aligned}a_1^{\Pi} &= \{(\lambda_2(s)+A(s))M_{\Pi}^0-B(s)M_{\gamma}^0\}\frac{1}{\lambda_2(s)-\lambda_1(s)}\\ a_2^{\Pi} &= M_0^{\Pi}-a_1^{\Pi}\\ a_1^{\gamma} &= \{(\lambda_2(s)+\sigma)M_{\gamma}^0-C(s)M_{\Pi}^0\}\frac{1}{\lambda_2(s)-\lambda_1(s)}\\ a_2^{\gamma} &= M_{\gamma}^0-a_1^{\gamma}\end{aligned} \tag{7.8}$$

corresponding to one initial electron of energy E_0

$$\Pi(E,0) = \delta(E-E_0) \qquad \gamma(E,0) = 0 \tag{7.9}$$

resulting in

$$M_{\gamma}^0(s) = E_0^s \qquad M_{\gamma}^0(s) = 0. \tag{7.10}$$

Numerical results of approximation A have been obtained from (7.3), neglecting contributions containing $\exp(\lambda_2(s)\,.\,t)$

$$\Pi(E,t) = \frac{1}{2\pi\mathrm{i}}\int_{s_0-\mathrm{i}\infty}^{s_0+\mathrm{i}\infty}\frac{\mathrm{d}s}{s}\left(\frac{E_0}{E}\right)^s a_1^{\Pi}(s)\exp(\lambda_1(s)\,.\,t) \tag{7.11}$$

by application of the saddle point method

$$\Pi(E,t)=\frac{(1/s_0)(E_0/E)^{s_0}a_1^{\Pi}(s_0)\exp(\lambda_1(s_0)\,.\,t)}{[2\pi\partial^2\ln\{(1/s_0)(E_0/E)^{s_0}a_1^{\Pi}(s_0)\exp(\lambda_1(s_0)\,.\,t)\}/\partial s_0^2]^{1/2}} \tag{7.12}$$

with s_0 taken from

$$0=\frac{\partial}{\partial s_0}\ln\left\{\frac{1}{s_0}\left(\frac{E_0}{E}\right)^{s_0}a_1^{\Pi}(s_0)\exp(\lambda_1(s_0)\,.\,t)\right\}. \tag{7.12a}$$

7.3. Review of approximation B

Cascade equations in approximation B include energy independent ionization loss

$$\frac{\partial}{\partial t}\Pi=-A'\Pi+B'\gamma+\epsilon\frac{\partial}{\partial E}\Pi \tag{7.13a}$$

$$\frac{\partial}{\partial t}\gamma=C'\Pi-\sigma\gamma. \tag{7.13b}$$

Solutions of these equations are given the form of Taylor series with respect to $\epsilon_1=\epsilon/E$

$$\Pi(E,t)=\sum_{n=0}^{\infty}(-\epsilon_1)^n\frac{1}{2\pi\mathrm{i}}\int_C \mathrm{d}s\,E^{-(s+1)}\Phi_n^{\Pi}(s,t) \tag{7.14a}$$

$$\gamma(E,t)=\sum_{n=0}^{\infty}(-\epsilon_1)^n\frac{1}{2\pi\mathrm{i}}\int_C \mathrm{d}s\,E^{-(s+1)}\Phi_n^{\gamma}(s,t). \tag{7.14b}$$

The lowest order approximation is

$$\Phi_0^{\Pi}(s,t)=M_{\Pi}(s,t) \tag{7.15a}$$

$$\Phi_0^{\gamma}(s,t)=M_{\gamma}(s,t). \tag{7.15b}$$

Introduction into the system of cascade equations and comparison of first order terms results in a system of equations which are difference equations with respect to s and differential equations with respect to t. Initial conditions are

$$\Phi_n^{\Pi}(s,0)=\Phi_n^{\gamma}(s,0)=0 \qquad \text{for } n>0. \tag{7.16}$$

The application of the Laplace transformation with respect to t results in recursion relations

$$\Phi_n^{\Pi}(s,p)=(s+n)\frac{p+\sigma}{(p-\lambda_1(s+n))(p-\lambda_2(s+n))}\Phi_{n-1}^{\Pi}(s,p) \tag{7.17a}$$

$$\Phi_n^{\gamma}(s,p)=(s+n)\frac{C(s+n)}{(p-\lambda_1(s+n))(p-\lambda_2(s+n))}\Phi_{n-1}^{\gamma}(s,p). \tag{7.17b}$$

If all terms with the exception of those containing $1/(p-\lambda_1(s))$ are neglected, the electron component is given by

$$\Phi_n^{\Pi}(s,p)=a_1^{\Pi}(s)\frac{\Gamma(s+n+1)}{\Gamma(s+1)}\frac{\mathcal{M}(s,n)}{p-\lambda_1(s)} \tag{7.18}$$

where $M(s, n)$ is determined by the recursion relation

$$M(s, n) = L^0(s, n) M(s, n-1) \tag{7.19}$$

with

$$L^0(s, n) = \frac{\lambda_1(s)+\sigma}{(\lambda_1(s)-\lambda_1(s+n))(\lambda_1(s)-\lambda_2(s+n))}. \tag{7.20}$$

The differential energy spectrum of electrons is thus found in the form

$$\Pi(E, t) = \sum_{n=0}^{\infty} (-\epsilon_1)^n \frac{1}{2\pi i} \int_C \mathrm{d}s\, E^{-(s+1)} a_1^{\Pi}(s) \frac{\Gamma(s+n+1)}{\Gamma(s+1)} M(s, n) \exp(\lambda_1(s) \cdot t) \tag{7.21}$$

within a range of convergence $0 \leqslant \epsilon_1 \leqslant \rho$. Analytical continuation of the solution is performed after transformation of the sum over discrete values of n into an integral over a continuous variable q within the region $|\arg(q)| \leqslant \pi/2$ of the complex q plane. For this purpose the function $M(s, n)$ is interpolated by means of an infinite product

$$M(s, q) = \frac{L^0(s+1)^{q+1}}{L^0(s+1+q)} \prod_{i=2}^{\infty} \frac{L^0(s+i)}{L^0(s+i+q)} \left(\frac{L^0(s+i)}{L^0(s+i-1)} \right)^q \tag{7.22}$$

which is in agreement with the former expression for all positive integer values of q. The function

$$\frac{1}{2\pi i} \int_C \mathrm{d}s\, E^{-(s+1)} a_1^{\Pi}(s) \epsilon_1^q \frac{\Gamma(1+s+q)}{\Gamma(1+s)} M(s, q) \exp(\lambda_1(s) \cdot t) \Gamma(-q) \Gamma(q+1) \tag{7.23}$$

is analytical within the half plane defined above with poles at the points $q = n$, the residues of which agree with the corresponding terms in the infinite sum over n. Therefore, (7.21) may be written in this form containing an integral over the continuous variable q along a path of integration around the aforementioned poles

$$\Pi(E, t) = \frac{1}{4\pi^2} \int_{Cs} \mathrm{d}s \frac{a_1^{\Pi}(s)}{E^{s+1}} \exp(\lambda_1(s) \cdot t) \int_{Cq} \frac{\mathrm{d}q}{1+(q/s)} \frac{\Gamma(s+1+q)}{\Gamma(s+1)} \Gamma(-q) \Gamma(q+1) M(s, q). \tag{7.24}$$

In our recalculations of approximation B, numerical results have been obtained by application of the double saddle point method to this expression.

7.4. Comparison of results from approximation B of conventional cascade theory with results of numerical integration using asymptotic cross sections and with results of numerical integration using exact cross sections

Figure 9(*a* and *b*) shows the integral energy spectrum of electrons in electron induced electromagnetic cascades in lead as a function of depth. Initial energies are $T_0 = 10^3$ MeV and 10^4 MeV. Full curves are results of numerical integration based on exact cross sections corresponding to different values of cut-off energy. Broken curves indicated by open circles represent results of numerical integration based on asymptotic cross sections, while broken curves indicated by crosses represent results obtained by means

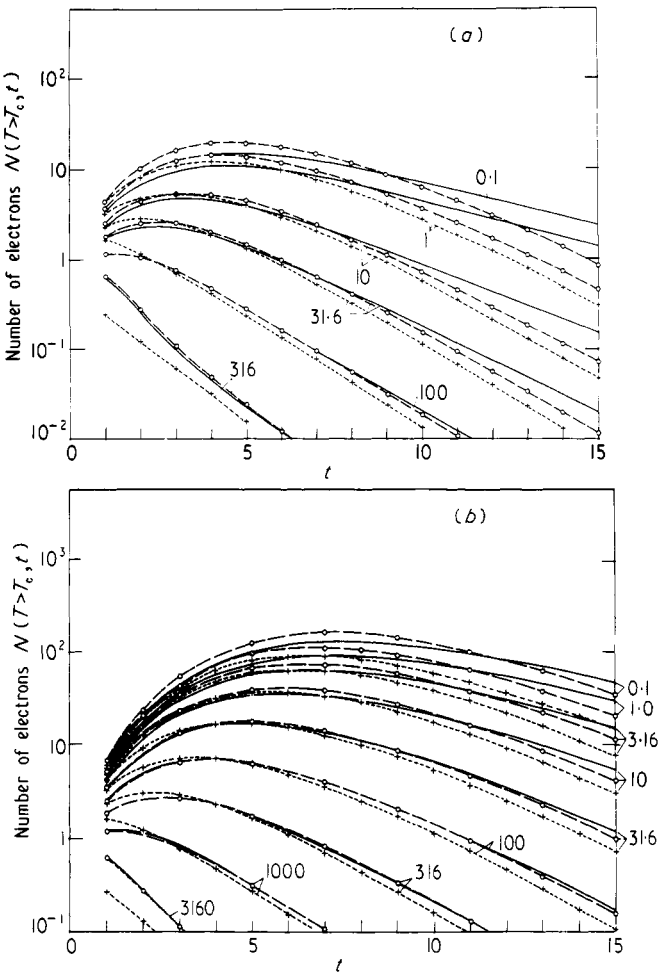

Figure 9. Transition curves of electrons in electron induced cascades in lead calculated with various assumptions. Full curves, numerical integration (exact cross sections); broken curves with open circles, numerical integration (asymptotic cross sections); broken curves with crosses, approximation B (asymptotic cross sections). Initial energies (MeV) are: (*a*) 10^3 and (*b*) 10^4. Different curves correspond to different values of T_c (MeV) in each part.

of approximation B. In the region of small depth, results of numerical integrations based on asymptotic cross sections are greater than those based on exact cross sections.

This is due to the different behaviour of exact and asymptotic differential interaction probabilities. In the region of cascade equilibrium at greater depth t, exact curves are steeper than asymptotic ones. This is a consequence of the fact, that total interaction probabilities are greater in their asymptotic form than in their exact form. This difference decreases with increasing initial energy. It is quite remarkable that these differences are much greater for photons than for electrons, as is demonstrated by figure 10(*a* and *b*).

Results obtained by means of approximation B tend to be parallel to those obtained by numerical integration based on asymptotic cross sections. Thus there is an almost constant relative error invoked by approximative methodical procedures in approximation B, which amounts to typically 10%.

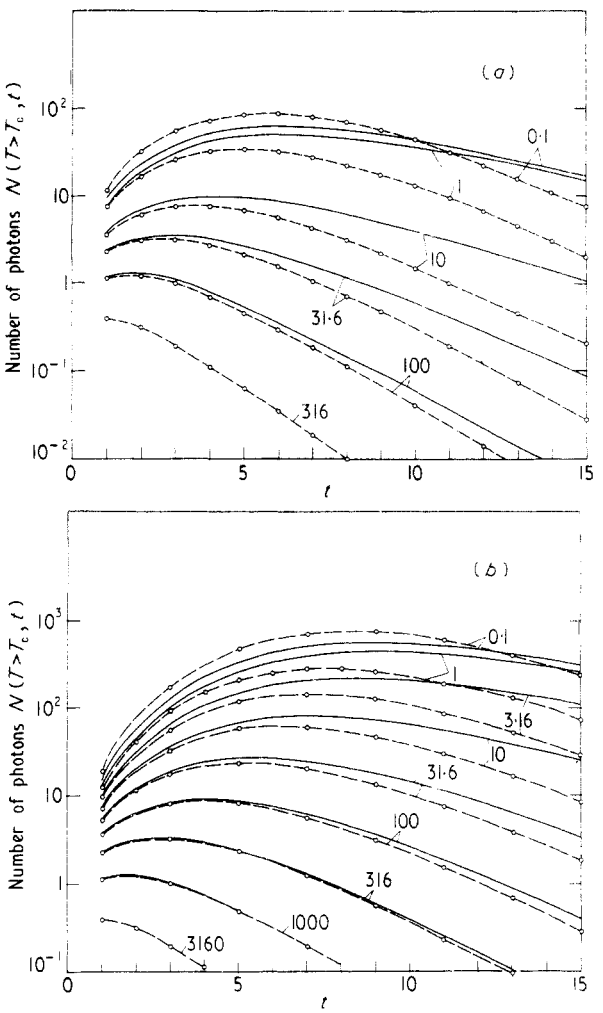

Figure 10. Transition curves of photons in electron induced cascades in lead calculated with various assumptions. Full curves, numerical integration (exact cross sections); broken curves with open circles, numerical integration (asymptotic cross sections). Initial energies (MeV) are: (*a*) 10^3 and (*b*) 10^4. Different curves correspond to different values of T_c (MeV) in each part.

7.5. Comparison of results from approximation A with those from approximation B of conventional cascade theory

In figure 11 the total number of electrons in electron induced electromagnetic cascades in lead is shown as a function of depth for different values of the decadic logarithm of the ratio of initial to cut-off energy. Results of approximation A tend to be greater than those of approximation B due to the neglection of ionization losses. This difference decreases with increasing values of initial and cut-off energies. There is an indication that results from approximation A are somewhat greater than results from approximation B for very high energies where different assumptions concerning cross sections are no longer important while approximative procedures involved in approximation B may result in greater systematic errors.

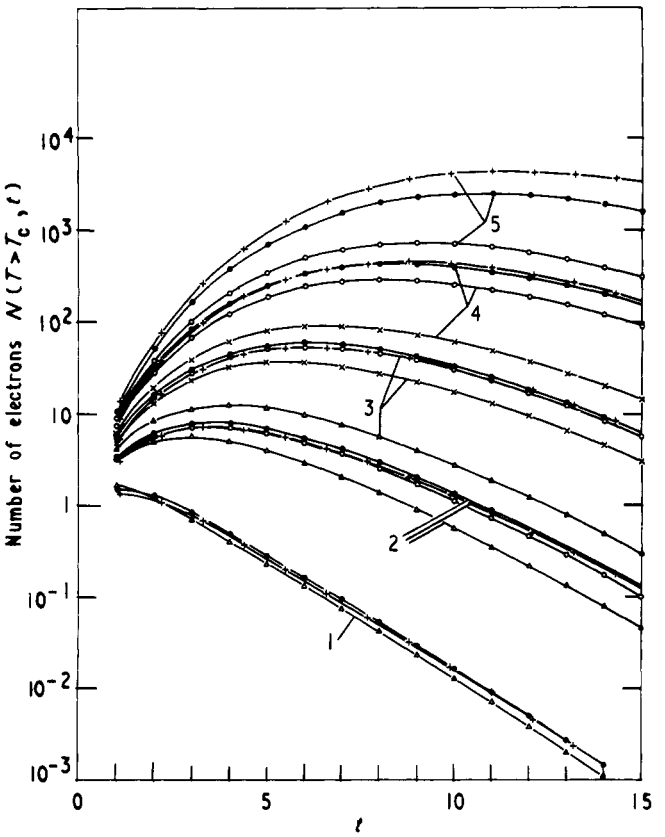

Figure 11. Total number of electrons in electron induced cascades in lead as functions of depth for different values of $\lg(T_0/T_c)$. + approximation A. ● $T_0 = 10^6$ MeV, ○ $T_0 = 10^5$ MeV, × $T_0 = 10^4$ MeV, △ $T_0 = 10^3$ MeV from approximation B.

8. Conclusions

Numerical data of the longitudinal development of electron induced electromagnetic cascades from numerical integration of cascade equations presented in graphical form for practical applications, are estimated to be accurate to about 1 % above several MeV, where the lateral divergence of cascades is of no importance. Comparison with data from Monte Carlo simulations and with experimental data shows full agreement.

We are therefore enabled to demonstrate the limits of applicability of approximations A and B of conventional cascade theory. In general, results from approximation B are less accurate for photons than for electrons in electron-induced cascades.

In comparison with the Monte Carlo procedure, the method of numerical integration proposed by us offers the advantages of slower increase of computing time with increasing initial energy and of the absence of statistical fluctuations in results.

Acknowledgments

The authors wish to acknowledge financial support by the Deutsche Forschungsgemeinschaft.

References

Becklin E E and Earl J A 1964 *Phys. Rev.* **136** B237–47
Bethe H A and Ashkin J 1953 *Experimental Nuclear Physics* ed E Segrè (New York: Wiley)
Bhabha H J 1936 *Proc. R. Soc.* A **154** 195–206
Bhabha H J and Chakrabarty S K 1943 *Proc. R .Soc.* **181** 267–301
—— 1948 *Phys. Rev.* **74** 1352–63
Bhabha H J and Heitler W 1937 *Proc. R. Soc.* **166** 432–58
Butcher J C and Messel H 1960 *Nucl. Phys.* **20** 15–128
Carlson J F and Oppenheimer J R 1936 *Phys. Rev.* **51** 220–31
Chakrabarty S K and Gupta M R 1956 *Phys. Rev.* **101** 813–9
Crannel C J 1967 *Phys. Rev.* **161** 310–21
Davis H, Bethe H A and Maximon L C 1954 *Phys. Rev.* **93** 788–95
Grodstein G N 1957 *Natn. Bur. Stand. Circ.* 583
Hall H 1936 *Rev. mod. Phys.* **8** 358–97
Heusch C A and Prescott C Y 1964 *Phys. Rev.* **135** B772–8
Klein O and Nishina Y 1929 *Z. Phys.* **52** 853
Koch H W and Motz W 1959 *Rev. mod. Phys.* **31** 920–55
Landau L and Rumer G 1938 *Proc. R. Soc.* **166** 213–28
Messel H and Crawford D 1970 *Tables* (Oxford: Pergamon)
Møller C 1932 *Ann. Phys.* **14** 531–85
Nagel H H 1965 *Z. Phys.* **186** 319–46
Nelson W R *et al* 1966 *Phys. Rev.* **149** 201–8
Nishimura J and Kamata K 1952 *Prog. theor. Phys.* **7** 185–92
Snyder H 1938 *Phys. Rev.* **53** 960–5
—— 1949 *Phys. Rev.* **76** 1563–71
Sternheimer R 1952 *Phys. Rev.* **88** 855–9
Thielheim K O and Zöllner R 1970a *Proc. 6th Inter-Am. Seminar on Cosmic Rays, La Paz* vol 4 11 pp 471–8
—— 1970b *Proc. 2nd European Symp. on Cosmic Rays, Leeds* 1970
—— 1971 *Proc. 12th Int. Conf. on Cosmic Rays, Hobart* (Hobart: University of Tasmania)
Thom H 1964 *Phys. Rev.* **136** B447–55
Volkel U 1965 *DESY Report* 6516
Wilson R R 1952 *Phys. Rev.* **86** 261–9
Zerby C D and Moran H S 1963 *J. appl. Phys.* **34** 2445–57